Research Article | Vol. 10, No. 8 / 1 August 2019 / Biomedical Optics Express 4159

Biomedical Optics EXPRESS

Single-pixel imaging of the retina through scattering media

RAHUL DUTTA,[1] SILVESTRE MANZANERA,[1] ADRIÁN GAMBÍN-REGADERA,[1] ESTHER IRLES,[2] ENRIQUE TAJAHUERCE,[2] JESÚS LANCIS,[2] AND PABLO ARTAL[1,*]

[1]*Laboratorio de Óptica, Instituto Universitario de Investigación en Óptica y Nanofísica, Universidad de Murcia, Campus de Espinardo (Edificio 34), E-30100, Murcia, Spain*

[2]*Institut of New Imaging Technologies, Universitat Jaume I, Castellon 12071, Spain*

[*]*pablo@um.es*

Abstract: Imaging the retina of cataractous patients is useful to detect pathologies before the cataract surgery is performed. However, for conventional ophthalmoscopes, opacifications convert the lens into a scattering medium that may greatly deteriorate the retinal image. In this paper we show, as a proof of concept, that it is possible to surpass the limitations imposed by scattering applying to both, a model and a healthy eye, a newly developed ophthalmoscope based on single-pixel imaging. To this end, an instrument was built that incorporates two imaging modalities: conventional flood illumination and single-pixel based. Images of the retina were acquired firstly in an artificial eye and later in healthy living eyes with different elements which replicate the scattering produced by cataractous lenses. Comparison between both types of imaging modalities shows that, under high levels of scattering, the single-pixel ophthalmoscope outperforms standard imaging methods.

1. Introduction

In recent times, single-pixel imaging has attracted significant attention as it provides some advantages over conventional imaging with pixelated detectors. In single-pixel imaging, the object is illuminated by a sequence of spatially structured images that form a basis in which any image can be decomposed. The total amount of light reflected or transmitted by the object is collected by a photodetector and the power measured for each image represents the coefficient for each component in the basis. Subsequently, a proper mathematical procedure allows for image reconstruction. It aids to build low-cost imaging system that operates outside the range of visible wavelengths. Single-pixel detectors find a wide range of applications in three-dimensional imaging [1], fluorescence microscopy [2], infrared imaging [3,4], and in ghost imaging [5,6]. On the other hand, imaging any object through a scattering or optically inhomogeneous media, like atmospheric turbulence or biological tissues, has been a long-standing problem with potential implications in the fields of biomedical imaging, navigation or remote sensing and several studies have been carried out lately providing new approaches to tackle this problem [7–11]. Relevant for this matter is the fact that single-pixel imaging has revealed to be robust to the presence of significant amounts of scattered light as demonstrated in recent works [12,13] showing images obtained through highly scattering biological tissues.

Based on this technique, a new instrument to image the fundus of the eye, named single-pixel camera ophthalmoscope, has been recently proposed [14]. A spatially structured illumination based on Hadamard patterns was projected onto the retina and the reflected intensity was measured by the photo detector in a double-pass configuration. This new instrument may be useful for retinal imaging in patients affected by cataracts. This is an ocular condition consisting in the opacification of the crystalline lens and is regarded as the main cause of blindness worldwide [15]. Although it is an age-related condition, there are some other factors, such as genetics,

#369258 https://doi.org/10.1364/BOE.10.004159
Journal © 2019 Received 4 Jun 2019; revised 12 Jul 2019; accepted 15 Jul 2019; published 19 Jul 2019

Biomedical Optics EXPRESS

diseases or nutritional deficiencies that may lead to the development of cataracts. The standard clinical procedure consists in the replacement of the natural lens with an artificial intraocular lens. In cases with severe opacifications in the lens the required exam of the retina cannot be carried out with standard ophthalmoscopes. Minkowski et al [16] described an instrument able to test the function of the retina in these patients. They measured visual acuity in patients with mild to moderate cataracts introducing a very narrow beam through clear areas in the lens without opacifications. Before, Green [17] used an alternative approach based in projecting interferences fringes into the retina. But to the best of our knowledge there is no instrument able to image the retina in patients with severe cataracts.

This paper demonstrates, as a proof of concept, that an ophthalmoscope based on single-pixel imaging outperforms standard ophthalmoscopes in the presence of a highly scattering media. A new instrument was built that incorporates two different optical paths to implement both types of ophthalmoscopes. Simple, but realistic simulations of cataract effects are performed for an artificial eye and healthy human eyes and images are compared. Our results provide useful insights into the challenges that need to be faced in retinal imaging of cataractous eyes.

2. Methods

2.1. Experimental setup

A schematic diagram of the experimental setup is illustrated in Fig. 1. This is a standard optical arrangement for ophthalmoscopy. The illumination system consists of a near infrared LED (Thorlabs M780LP1, Newton, NJ, USA) whose light is coupled into a light pipe that produces a homogeneous light source illuminating a digital micromirror DMD (Vialux V7001, Chemnitz, Germany).

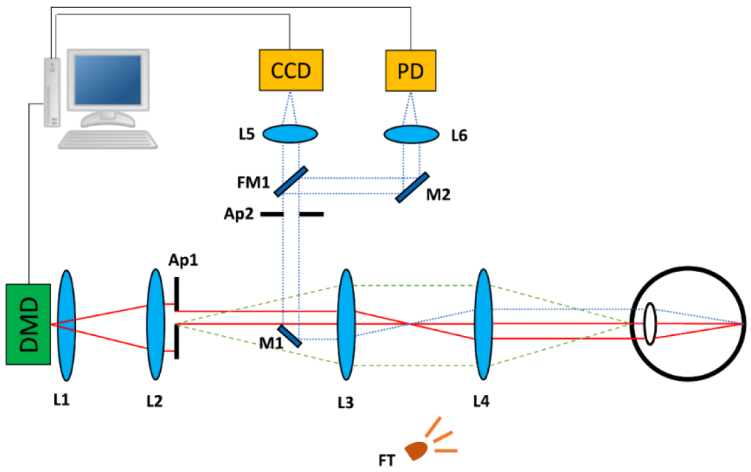

Fig. 1. Schematic diagram of the optical setup (the light source and the light beam illuminating the DMD have been omitted). The Hadamard patterns generated on the DMD are imaged onto the retina as shown by the solid red line. The reflected light beam from the retina is depicted by a dotted blue line reaching either the CCD camera or the photodetector (PD) by means of the flip mirror FM1. The apertures (Ap1 and Ap2) are conjugated with the pupil plane of the eye (green dashed line). L1 to L6 denote lenses, M1 to M2 mirrors and FT stands for fixation target.

A sequence of 2D binary (black and white) patterns, which are the full set of functions of the Walsh-Hadamard basis for the considered resolution, are generated using an in-house developed software in C++ and sent to the DMD's onboard memory using a USB 3.0 connection. This

Biomedical Optics EXPRESS

pre-loading operation is necessary to achieve the maximum frequency of the DMD, which is 22.7 kHz. The sequence of patterns is then displayed at maximum speed. The light reflected from each micro-mirror on the DMD is guided through the optical system as described later and the generated Hadamard patterns are projected onto the retina. The LED has peak wavelength of 780 nm with 30-nm bandwidth providing a maximum power of 260 μW at the pupil plane which is well below safety limits (2 mW in this case, ANSI Z136.1-2014). This source produces stable output over time, which is prerequisite for discriminating small intensity changes arising from the spatially coded Hadamard patterns. The sequence of patterns is initialized within an area of 512×512 pixels in the center of the DMD. The images are scaled to match the size on the DMD according to the resolution of the output image, i.e., for a resolution of 64×64, each pixel of the pattern corresponds to 8×8 pixels on the DMD. In this configuration we can image an 18-degrees square patch of the retina.

Figure 1 depicts how the Hadamard patterns are imaged onto the retina after passing through the lenses L1 and L2, the 4-f system formed by lenses L3 and L4, and the optics of the eye. A 2×2-mm aperture (Ap1), conjugated with the eye's pupil plane, is placed at a focal distance from lens L3 and above the optical axis, thereby selecting the lower part of the eye's pupil as the location of light entry into the eye. The reflected light beam from the retina is collected by the same 4-f system and is guided to the detectors through the mirror M1, placed below the optical axis. The detection channel consists of 2 different optical paths which allows, by means of the flip mirror FM1, to image the retina using either a CCD camera (conventional ophthalmoscope) or a photodetector (single-pixel based ophthalmoscope). The camera is a model Luca R604 (Andor Technology, Belfast, UK) and the photodetector is a hybrid model (R10467U-50-01; Hamamatsu City, Japan). A second 7×2-mm aperture (Ap2) is optically conjugated with the pupil plane. This aperture and the mirror M1 work together to select only light that is departing from the pupil exclusively from the upper part. The arrangement of apertures Ap1 and Ap2 and the mirror M1 avoid the corneal reflection from the incoming beam. In addition, the small size of Ap1 helps to produce a nearly diffraction limited image of the structured patterns on the retina. Further details regarding the software and the control system can be found elsewhere [14].

The fixation target (FT) is simply a LED that is perceived by the volunteer as a small, orange colored spot and is used to fixate the imaged retinal area. Placed on the left-hand side of the volunteer's line of sight (from the volunteer's perspective), it allows to image the optic disk of the right eye. In addition to the fixation target, volunteer's movements are limited by the use of a dental impression.

2.2. Simulation of the cataract effects in a model and a healthy human eye

Figure 2 shows two OCT images of crystalline lenses affected by cataract [18,19]. Some regions remain transparent with the spatial distribution depending on the type of cataract.

We have made use of this nonuniformity in the distribution of opacities to simulate the effect of a cataractous lens. In the first place we have employed an artificial eye consisting of a lens (20-mm focal length) and a piece of paper with printed letters acting as the retina. The cataract effects have been introduced in two different ways. Firstly, some semi-transparent random patterns are drawn with glue on a plastic film so that the region of interest depicts some transparency in the midst of the opacity. In the second approach, we have considered a piece of paper, which is regarded a strong scattering medium, with a 2×2-mm aperture on it. To simulate realistic cataract cases, we have placed the film or the paper in front of the focusing lens of the artificial eye, close to the pupil plane. An image of both elements is shown in Fig. 3. The film or the piece of paper are placed in such a way that they permit the incoming beam to pass through the unobstructed regions of the element.

Before imaging eyes affected by cataracts, we decided, for simplicity, to obtain retinal images of healthy volunteers simulating the scattering produced by a cataractous lens. We have considered

Biomedical Optics EXPRESS

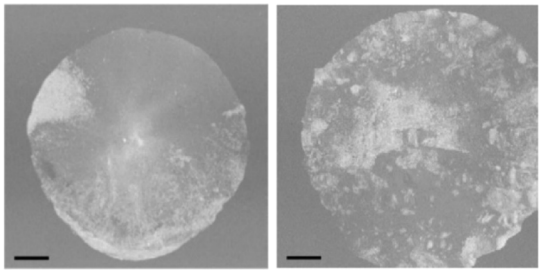

Fig. 2. OCT projection images of crystalline lenses in cataract patients. Both images correspond to 2 females, 53(left) and 63(right) years old. *Scale bars*: 1 mm.

Fig. 3. Crude approaches to simulate the cataract effects with a model eye. Some random patterns drawn on a plastic thin film using glue (left) and a piece of paper with a 2 mm aperture (right). The scale bar on the left represents 5 mm.

an alternative approach to induce scatter in which the diffusing element is placed next to aperture Ap2, in an optically conjugated plane with the eye's pupil. Note that in this configuration the incoming beam into the eye does not suffer any scattering and only reflected light from the retina experiences the scattering medium. This situation is not actually different to that simulated for the artificial eye. Figure 4 shows an image of the diffusing element employed, a circular plate made of silicone, 2-mm thick.

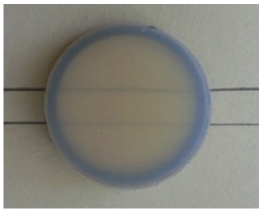

Fig. 4. Diffuser used to simulate cataracts in a healthy eye. It is a 2-mm thick plate of silicone. In the picture, the plate is 2 mm above the drawing of the 2 parallel lines.

One volunteer participated in the experiment, a male, 30 years old, emmetrope and with no record of ocular disease. The experiment complied with the tenets of the declaration of Helsinki and it was carried out after the corresponding informed consent was signed.

Biomedical Optics EXPRESS

3. Results

3.1. Artificial eye

Figure 5 shows the images of the artificial retina in the absence of any scattering medium provided by the CCD and that recorded by the single-pixel camera with a resolution of 64×64 pixels, the latter rescaled to match the size of the former. Except for the obvious higher resolution of the image obtained directly with the CCD, both images are similar, with no significant difference in contrast. Light intensity, exposure time and gain of the CCD camera were adjusted to produce similar images that could serve as a baseline.

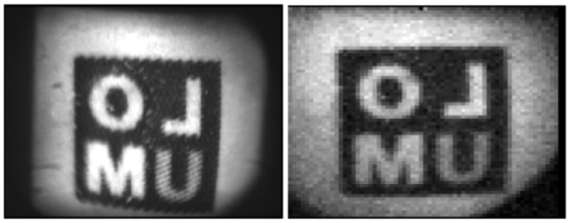

Fig. 5. Images of the retina in the model eye in the absence of any scattering medium recorded by the CCD (left) and by the single-pixel camera (right). Field size of the illuminated area is 18×18 degrees.

Next, we simulated the cataracts effect by placing the plastic film with glue at the pupil plane of the artificial eye and moving it a bit so that the reflected light from the retina experiences different opacities present on the film. The film is positioned in such a way that the incoming beam always pass through the transparent part of it. The subsequent images recorded by the CCD and the single-pixel camera are illustrated in Fig. 6 showing how image quality for the CCD camera is limited in different ways by the opacities whereas it remains fairly stable for the single-pixel camera in all cases.

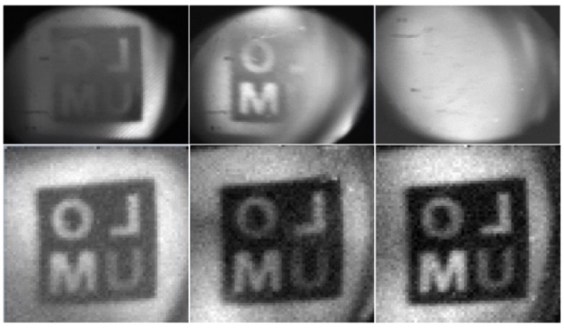

Fig. 6. Retinal images of the artificial eye after simulating the cataract effect using a plastic film with glue. Along each column are shown the corresponding CCD (upper row) and single pixel images (lower row) captured for different locations of the plastic film. Field size is 18×18 degrees.

In addition, we have demonstrated similar results with a stronger opaque medium. Here we have used the piece of paper with a small aperture as described in the previous section allowing the incoming beam to the model eye to pass unobstructed but limiting a big deal of the outcoming one. The images of the retina recorded by the CCD and the single-pixel camera are shown in Fig. 7. In this case, no details at all can be observed in the image from the CCD whereas for

Biomedical Optics EXPRESS

the single-pixel camera the main features of the image are still visible. Obviously, this image is noisier than that exhibited in Fig. 6 as the scattering effect of the new element is much stronger.

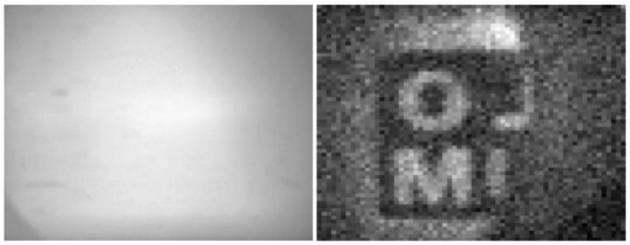

Fig. 7. Images of the retina in the model eye in the presence of a strong scattering medium. CCD (left), single-pixel camera (right). The medium is a piece of paper with a 2-mm aperture allowing the incoming beam to pass unobstructed but limiting the outcoming one. Field size is 18×18 degrees.

3.2. Living eye

After successful comparison in an artificial eye of the images produced by conventional and single-pixel ophthalmoscopes in the presence of a scattering medium, we took a step further and performed a similar comparison in the living human eye. Initially, we recorded retinal images without any element producing light diffusion in the system. They are presented in Fig. 8 and show the optics disk of a healthy volunteer covering a square patch on the retina of 18 degrees each side. As in the case of the model eye, images from the single-pixel camera are obtained with a resolution of 64×64 pixels and rescaled in size to make possible the comparison with the CCD camera images. For the living eye the conventional imaging outperforms the single-pixel approach mostly due to the longer exposure time required (360 ms), which makes eye movements a relevant factor diminishing the image quality. The lower resolution makes difficult to discern fine retinal structures as well. But the optics disk is clearly visible and the images are adequate to test the robustness of both approaches to diffusing elements. To specifically image the retinal area surrounding the optic disk, the operator used the real-time images provided by the CCD camera and asked the volunteer to follow the fixation target (FT) until the optic disk was on the center of the image.

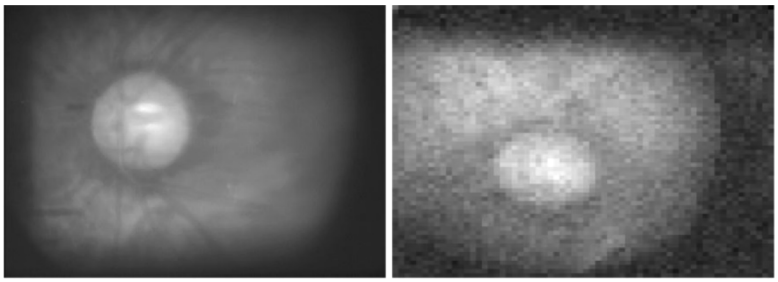

Fig. 8. Fundus images of a healthy eye captured by the CCD (left) and the single-pixel camera (right) showing the surroundings of the optic disk. Imaged area is a 18×18 degrees patch. Single-pixel image resolution is 64×64 pixels and is rescaled in size.

The silicon plate shown in Fig. 4 was placed in the pupil-conjugated plane in front of both detectors, next to aperture Ap2, and the same retinal area of the same volunteer was imaged. Figure 9 exhibits the corresponding images acquired using the CCD and the single-pixel cameras.

Biomedical Optics EXPRESS

The silicon plate is a highly scattering medium that makes impossible to discern any feature in the image captured by the CCD camera. However, although noisier, the image recorded by the single-pixel approach still allows for locating the brighter, round-like shape of the optic disk.

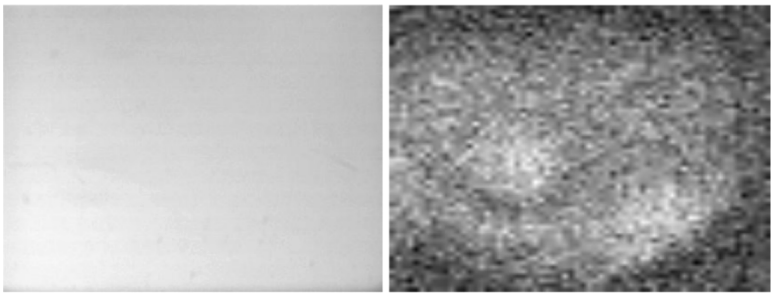

Fig. 9. Retinal images aiming at the optic disk obtained after simulating the cataract effect placing a strong diffuser in the path of both detectors, CCD camera (left image) and photodetector (right image) for the single-pixel camera. Imaged area is a 18×18 degrees patch. Single-pixel image resolution is 64×64 pixels and is rescaled in size.

4. Discussion and conclusions

Tajahuerce et al. demonstrated [12] that it was possible to image objects hidden behind layers of scattering media by making use of the single-pixel imaging technique. Those results suggested the opportunity to solve a long-standing problem in Ophthalmology consisting in the impossibility of obtaining fundus images in cataractous patients. Lochocki et al. [14] took the first step demonstrating the first single-pixel based ophthalmoscope. In this work we have taken a step further, showing that, in addition, this approach ophthalmoscope is able to provide retinal images under high scattering conditions, whereas a standard ophthalmoscope, based on CCD cameras, fails to do so. Retinal images obtained in the presence of scattering elements that simulate a cataractous crystalline lens in both, a model eye and the eye of a healthy volunteer, have been presented. There are still some issues that need to be solved before the instrument can be used in a clinical setting. The first of them is that the robustness to scattering is partly based on the requirement that the spatially coded binary patterns need to be sharply imaged onto the retina. For a healthy eye, only refractive error and ocular aberrations play a significant role that can be easily solved (reducing the size of the incoming beam), but for a cataractous eye the opacities in the lens scatter light in the way into the eye reducing the sharpness of the binary pattern. The nonuniform arrangement of these opacities leaves unobstructed areas that could be used to solve this problem. The same advantage was previously used by Minkowski et al [16] and Green [17] to deliver a pencil of light to the retina and test visual acuity. In the experiment using the healthy living eye the scattering element was placed only in the path of the outcoming beam, assuming that for a cataractous patient, we could avoid the opacities in the incoming way. The second group of factors limiting the performance of the single-pixel ophthalmoscope are of a technical nature. The achievable image resolution and the needed time to obtain an image are linked by an exponential relationship. The 64×64 pixels resolution used in our experiment requires of a 360-ms exposure time which could allows that eye movements degrade the retinal image. In this case, the limitation arises from the current state of the art in DMDs that, to our knowledge, does not allow to run these devices at refresh rates higher than 22.7 kHz. To ameliorate the effect of movements on image quality during such a relatively long exposure time, the use of a bitebar to keep the head stable and a fixation target to minimize eye movements is required. Another dynamic source of noise may be pupil size, although not relevant changes are expected during the 360-ms duration of the measurement. In case they exist, the effect would be that the

Biomedical Optics EXPRESS

amount of light collected for each light pattern would be affected by the different pupil size and the reconstructed image would be noisier. However, the arrangement of apertures Ap1 and Ap2 in the optical setup acts as an artificial pupil that limit the effect of changes in the natural pupil, always assumed that the later is larger than the former. Other limiting factor is the detection of the weak light intensity reflected from the retina for each of the displayed binary patterns. To compensate for this, the gain in the photodetector must be increased with the consequent decrement in the signal-to-noise ratio.

In conclusion, we have developed a dual, standard and single-pixel based, ophthalmoscope that has been used to demonstrate the highest performance of the latter to obtain retinal images under the presence of high levels of scattering in the path of the outcoming beam from the retina to the detector. Although some technical issues limit its current applicability in the clinic, this work serves as a proof of concept to show the potential of this technique.

Funding

H2020 European Research Council (ERC) (ERC-2013-AdG-339228); Secretaría de Estado de Investigación, Desarrollo e Innovación (SEIDI) (FIS2016-75618-R, FIS2016-76163-R)); Fundación Séneca (f SéNeCa) (19897/GERM/15).

Disclosures

The authors declare that there are no conflicts of interest related to this article.

References

1. B. Sun, M. P. Edgar, R. Bowman, L. E. Vittert, S. Welsh, A. Bowman, and M. J. Padgett, "3D Computational Imaging with Single-Pixel Detectors - Supplementary Materials," Science **340**(6134), 844–847 (2013).
2. V. Studer, J. Bobin, M. Chahid, H. S. Mousavi, E. Candes, and M. Dahan, "Compressive fluorescence microscopy for biological and hyperspectral imaging," Proc. Natl. Acad. Sci. **109**(26), E1679–E1687 (2012).
3. M. P. Edgar, G. M. Gibson, R. W. Bowman, B. Sun, N. Radwell, K. J. Mitchell, S. S. Welsh, and M. J. Padgett, "Simultaneous real-time visible and infrared video with single-pixel detectors," Sci. Rep. **5**(1), 10669 (2015).
4. H. Peng, Z. Yang, D. Li, and L. Wu, "The application of ghost imaging in infrared imaging detection technology," in *Selected Papers of the Photoelectronic Technology Committee Conferences*, S. Liu, S. Zhuang, M. I. Petelin, and L. Xiang, eds. (International Society for Optics and Photonics, 2015), Vol. 9795, p. 97952O.
5. Y. Bromberg, O. Katz, and Y. Silberberg, "Ghost imaging with a single detector," Phys. Rev. A: At., Mol., Opt. Phys. **79**(5), 053840 (2009).
6. P. Clemente, V. Durán, E. Tajahuerce, V. Torres-Company, and J. Lancis, "Single-pixel digital ghost holography," Phys. Rev. A: At., Mol., Opt. Phys. **86**(4), 041803 (2012).
7. S. Popoff, G. Lerosey, M. Fink, A. C. Boccara, and S. Gigan, "Image transmission through an opaque material," Nat. Commun. **1**(1), 81 (2010).
8. J. Bertolotti, E. G. Van Putten, C. Blum, A. Lagendijk, W. L. Vos, and A. P. Mosk, "Non-invasive imaging through opaque scattering layers," Nature **491**(7423), 232–234 (2012).
9. J. A. Newman and K. J. Webb, "Imaging optical fields through heavily scattering media," Phys. Rev. Lett. **113**(26), 263903 (2014).
10. O. Katz, P. Heidmann, M. Fink, and S. Gigan, "Non-invasive single-shot imaging through scattering layers and around corners via speckle correlations," Nat. Photonics **8**(10), 784–790 (2014).
11. S. Sudarsanam, J. Mathew, S. Panigrahi, J. Fade, M. Alouini, and H. Ramachandran, "Real-time imaging through strongly scattering media: Seeing through turbid media, instantly," Sci. Rep. **6**(1), 25033–9 (2016).
12. E. Tajahuerce, V. Dur, P. Clemente, E. Irles, F. Soldevila, and P. Andr, "Image transmission through dynamic scattering media by single-pixel photodetection," Opt. Express **22**(14), 16945–16955 (2014).
13. V. Durán, F. Soldevila, E. Irles, P. Clemente, E. Tajahuerce, P. Andrés, and J. Lancis, "Compressive imaging in scattering media," Opt. Express **23**(11), 14424 (2015).
14. B. Lochocki, A. Gambín, S. Manzanera, E. Irles, E. Tajahuerce, J. Lancis, and P. Artal, "Single pixel camera ophthalmoscope," Optica **3**(10), 1056–1059 (2016).
15. B. Thylefors, "The World Health Organization's programme for the prevention of blindness," Int. Ophthalmol. **14**(3), 211–219 (1990).
16. J. S. Minkowski, M. Palese, and D. L. Guyton, "Potential Acuity Meter Using a Minute Aerial Pinhole Aperture," Ophthalmology **90**(11), 1360–1368 (1983).
17. D. G. Green, "Testing the Vision of Cataract Patients by Means of Laser-Generated Interference Fringes," Science **168**(3936), 1240–1242 (1970).

Biomedical Optics EXPRESS

18. A. de Castro, A. Benito, S. Manzanera, J. Mompeán, B. Cañizares, D. Martínez, J. M. Marín, I. Grulkowski, and P. Artal, "Three-dimensional cataract crystalline lens imaging with swept-source optical coherence tomography," Invest. Ophthalmol. Visual Sci. **59**(2), 897–903 (2018).
19. I. Grulkowski, S. Manzanera, L. Cwiklinski, J. Mompeán, A. DeCastro, J. M. Marin, and P. Artal, "Volumetric macro- and micro-scale assessment of crystalline lens opacities in cataract patients using long-depth-range swept source optical coherence tomography," Biomed. Opt. Express **9**(8), 3821–3833 (2018).